

**Conformational Equilibria of  
7-Benzyl-2-iodo-9-oxa-7-azabicyclo[4.3.0]nonan-8-one in Solution.  
Correlations between Conformational Distribution and Solvent  
Solvatochromic Parameters**

Esther Vaz, Isabelle Fernández, and Luis Muñoz\*

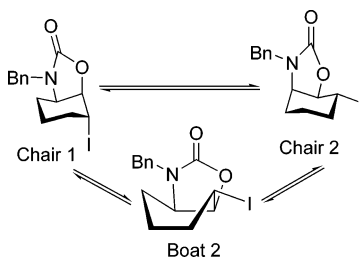
*Departamento de Química Orgánica, Facultad de Química, Universidade de Vigo, 36310 Vigo, Spain*

Juan Llor\*

*Departamento de Química Física, Facultad de Ciencias, Universidad de Granada, 18003 Granada, Spain*

*lmunoz@wigo.es*

*Received September 13, 2005*



A quantitative study of the variation of the conformational equilibria of 7-benzyl-2-iodo-9-oxa-7-azabicyclo[4.3.0]nonan-8-one **1** in 10 solvents has been carried out. The experimental composition in each solvent has been obtained from experimental NMR vicinal H–H coupling constants together with molecular modeling. The solvent properties, particularly polarity and hydrogen bonding ability, were described according to Kamlet and Taft using experimental parameters. Very good linear relationships were obtained between the equilibrium constants of each single conformational equilibrium and the polarity and hydrogen bonding parameters of the solvent. These linear relationships allow an accurate prediction of the conformational composition in any solvent as well as a thorough understanding of the influence of each separate parameter on the conformational equilibrium composition.

**Introduction**

Changing the medium can have particular effects on various conformational and rotational equilibria. Given that the Gibbs energy differences between conformational isomers are almost always very small (ca. 0–13 kJ/mol) and the solvation enthalpies of dipolar solutes are at least as large as this (and often much larger), the medium can affect conformational equilibria to a great extent. It is clearly important to obtain a detailed understanding of solvent effects on conformational equilibria because they may have profound consequences on the chemical nature and behavior of a system. These effects result from the sum of the interaction forces between the solvent and solute molecules.

Numerous attempts have been made to calculate relative conformer energies in solution, using physical properties of solutes and solvents, to derive theoretical procedures or models

with predictive ability. The methods employed include quantum-chemical calculations,<sup>1</sup> statistical mechanics and molecular dynamics calculations,<sup>2</sup> and reaction field methods based on Onsager's theory of dipolar molecules in the condensed phase.<sup>3,4</sup> However, these methods suffer from significant drawbacks in terms of describing specific solute/solvent interactions such as hydrogen bonding and quadrupole or higher multipole moments of solvent molecules.<sup>5</sup> Moreover, theoretical modeling may not

- (1) Dietz, F.; Förster, W.; Thieme, R.; Weiss, C. *Z. Chem.* **1982**, *22*, 144.
- (2) Jorgensen, J. L. *J. Phys. Chem.* **1983**, *87*, 5304.
- (3) Abraham, R. J.; Bretschneider, E. Medium Effects on Rotational and Conformational Equilibria. In *Internal Rotation in Molecules*; Orville-Thomas, W. J., Ed.; Wiley-Interscience: New York, 1974.
- (4) Dosen-Micovic, L.; Zigman, V. *J. Chem. Soc., Perkin Trans. 2* **1985**, 625.
- (5) Reichardt, C. *Angew. Chem., Int. Ed. Engl.* **1965**, *4*, 29.

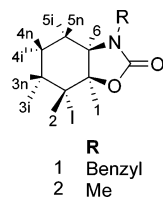


**FIGURE 1.** Compounds **1** and **2** (protons are labeled i (syn with I) and n (syn with N)).

provide solvent effects for a given equilibrium because of the necessity of taking into account all the specific and nonspecific intermolecular forces between solvent and solute molecules (Coulomb interactions between ions, directional interactions between dipoles, inductive, dispersion, hydrogen bonding, charge-transfer forces, and solvophobic interactions).

These shortcomings have stimulated attempts to introduce empirical scales of solvent polarity<sup>6</sup> based on solvent-sensitive reference processes. One example of a successful quantitative treatment of solvent effects using a multiparameter equation was described by Kamlet and Taft<sup>7–9</sup> and is known as the linear solvation energy relationship (LSER). The equation developed by Kamlet and Taft explains the variation of the properties of any solute with solvent composition in terms of a linear combination of the microscopic parameters of the solvent ( $\pi^*$ ,  $\alpha$ , and  $\beta$ ). The solvatochromic parameter  $\pi^*$  is an index of solvent dipolarity/polarizability, which measures the ability of the solvent to stabilize a charge or a dipole by virtue of its dielectric effect. Parameter  $\alpha$  is a quantitative, empirical measurement of the solvent hydrogen-bond donor (HBD) acidity and describes the ability of a solvent to donate a proton in a solvent–solute hydrogen bond. Finally,  $\beta$  is a measure of the solvent's hydrogen-bond acceptor (HBA) basicity and describes the ability of the solvent to accept a proton (or, vice versa, to donate an electron pair) in a solute–solvent hydrogen bond. The solvatochromic comparison method, introduced by Kamlet and Taft<sup>7–9</sup> and further developed by Abboud and Abraham,<sup>9</sup> makes use of eq 1:

$$Y(s) = Y(o) + a\alpha + b\beta + s\pi^* \quad (1)$$

where  $Y(s)$  and  $Y(o)$  represent the solute property in question in a given solvent and in a solvent for which  $\alpha = \beta = \pi^* = 0$ ; and  $a$ ,  $b$ , and  $s$  are the respective susceptibilities of the solute property to changes in the  $\alpha$ ,  $\beta$ , and  $\pi^*$  values of the solvent. Equation 1 is a simplification of the generalized solvatochromic equation.<sup>9</sup>

The high-resolution <sup>1</sup>H NMR spectra of compound **1** (Figure 1) show remarkable variations in different solvents. Careful analysis showed that the signals corresponding to the cyclohexane ring exhibit strong solvent dependence that affected

chemical shifts as well as the magnitude of spin–spin coupling constants ( $J_{\text{HH}}$ ). These changes can be understood in terms of a fluctuation in the conformational equilibrium due to medium effects. We therefore decided to study the conformational distribution of bicyclic oxazolidinone **1** in different solvents and to ascertain how this conformational isomerism is related to medium effects. Analysis of the conformational populations in different solvents enabled us to establish mathematical correlations between the equilibrium composition and empirical solvent parameters. These correlations in turn allow the prediction of the equilibrium behavior of the substrate in the solution.

## Results and Discussion

Experimental chemical shifts ( $\delta$ ) and coupling constants ( $J_{\text{exp}}$ ) were obtained for racemic compound **1** in 10 solvents, acetic acid-*d*<sub>4</sub>, acetone-*d*<sub>6</sub>, acetonitrile-*d*<sub>3</sub>, benzene-*d*<sub>6</sub>, CCl<sub>4</sub>, CDCl<sub>3</sub>-*d*<sub>3</sub>, DMSO-*d*<sub>6</sub>, MeOH-*d*<sub>4</sub>, pyridine-*d*<sub>5</sub>, and toluene-*d*<sub>8</sub>, by the iterative fitting of the simulated <sup>1</sup>H NMR spectrum to the experimental one. The set of solvents was selected to represent a wide range of properties such as polarity and ability to form hydrogen bonds. Only the nine-proton spin system corresponding to the cyclohexane ring was used for the iteration. In this way, 14 vicinal, 3 geminal, and 1 four-bond coupling constants were obtained in each solvent. The experimental and iterated spectra of **1** in acetone-*d*<sub>6</sub> are shown in the Supporting Information, and the experimental vicinal coupling constants in each solvent, as they were obtained from the iteration output, are given in Table 1. The variation of three-bond  $J$  values can be ascribed to a variation in the conformational equilibrium due to the different interactions between compound **1** and each solvent.

The NMR signals were assigned on the basis of standard 2D NMR experiments. The spin system was easily determined through standard COSY, HSQC, and HMBC experiments. The stereochemistry of each methylene proton was determined through a NOESY correlation in chloroform and DMSO. In an effort to clarify the stereochemistries of the cyclohexane protons, each proton in each methylene was labeled with an i or n subscript added to the position number indicating a syn arrangement between the given proton and the iodo substituent or the nitrogen, respectively (Figure 1). The stereochemical assignment was later confirmed by the correlation coefficients of the fitting calculation.

A theoretical conformational analysis was carried out for the bicyclic ring system. Although the oxazolidinone ring is rigid and nearly flat, the cyclohexane ring was found to be unusually dynamic. In addition to the two ordinary chair conformers, a few twist-boat conformations proved to be significant. In an attempt to reduce the conformational space and the calculation time, the benzyl group of **1** was replaced by a methyl group (**2**) in the minimization calculation. Accordingly, the cyclohexane ring of compound **2** was modeled by several methods at different levels of theory, ranging from molecular mechanics to DFT. The reason for this approach is that orbital d atoms such as iodine are not well parametrized by molecular mechanics. Therefore, in principle, more sophisticated methods should give better results. Six minimum energy conformations were found: two chairs (chair 1 and chair 2) and two boats (boat 1 and boat 2), each of which is twisted in the two possible rotational ways (Figure 2). The manner of rotation was labeled (+) or (–) depending on the sign of the angle produced in an extended Newman projection by the two axial bonds on C2 and C5. One of the chairs and two twist-boats have an axial iodo substituent,

(6) (a) Reichardt, C. In *Organic Liquids – Structure, Dynamics and Chemical Properties*; Buckingham, A. D., Lippert, E., Bratos, E., Eds.; Wiley: New York, 1978; pp 269–291. (b) Abboud, J.-L. M.; Kamlet, M. J.; Taft, R. W. *Prog. Phys. Org. Chem.* **1981**, *13*, 485. (c) Bentley, T. W.; Llewellyn, G. *Prog. Phys. Org. Chem.* **1990**, *17*, 121. (d) Buncl, E.; Rajagopal, S. *Acc. Chem. Res.* **1990**, *23*, 226. (e) Laurence, C. In *Similarity Models in Organic Chemistry, Biochemistry and Related Fields*; Zalewski, R. I., Krygowski, T. M., Shorter, J., Eds.; Elsevier: Amsterdam, 1991; Chapter 5, pp 231–281. (f) Fawcett, W. R. *J. Phys. Chem.* **1993**, *97*, 9540.

(7) Kamlet, M. J.; Taft, R. W. *J. Am. Chem. Soc.* **1976**, *98*, 2886.

(8) Kamlet, M. J.; Abboud, J. L.; Taft, R. W. *J. Am. Chem. Soc.* **1977**, *99*, 6027.

(9) Kamlet, M. J.; Abboud, J. L. M.; Abraham, M. H.; Taft, R. W. *J. Org. Chem.* **1983**, *48*, 2877.

**TABLE 1.** Experimental Three-Bond Coupling Constants ( $^3J_{\text{exp}}$ , Hz) in Ten Deuterated Solvents

	acetic acid	acetone	acetonitrile	benzene	CCl <sub>4</sub>	chloroform	DMSO	methanol	pyridine	toluene
H1–H2	7.22	8.23	8.34	7.02	5.81	6.43	8.57	8.03	7.78	7.09
H1–H6	6.96	6.74	6.74	6.78	5.89	6.43	6.94	6.86	6.86	6.41
H2–H3n	4.27	4.42	4.60	4.22	3.94	3.93	4.45	4.57	4.44	4.15
H2–H3i	10.52	11.76	11.72	10.15	8.02	9.04	12.07	11.40	11.48	10.00
H6–H5n	4.68	3.94	4.15	5.17	5.75	5.49	3.86	3.94	4.36	5.27
H6–H5i	4.85	4.61	4.39	4.86	5.44	5.20	4.52	4.58	4.56	5.12
H3n–H3i	–14.03	–13.51	–13.70	–14.00	–14.55	–14.45	–13.39	–13.80	–13.85	–13.94
H3n–H4i	5.65	4.40	4.85	5.91	7.78	7.19	4.44	4.95	4.55	6.23
H3n–H4n	4.14	4.28	3.71	3.91	3.57	3.88	3.76	3.70	4.38	3.66
H3i–H4i	3.71	3.43	3.70	3.76	3.80	3.81	3.79	3.75	3.19	3.78
H3i–H4n	10.31	11.45	11.00	10.24	8.52	9.10	11.25	10.82	11.22	10.03
H4i–H4n	–14.30	–14.37	–14.28	–14.12	–14.25	–13.98	–14.00	–14.28	–14.19	–14.11
H4i–H5n	6.33	4.19	4.42	4.30	7.51	7.40	4.16	5.16	4.52	4.99
H4i–H5i	4.50	4.56	4.48	5.32	4.36	4.23	4.42	4.50	4.45	4.83
H4n–H5n	3.89	3.91	3.65	4.14	4.07	4.16	3.84	3.73	4.18	4.81
H4n–H5i	10.55	11.78	11.51	10.06	9.00	10.02	11.54	11.26	11.01	9.92
H5n–H5i	–14.99	–15.07	–15.43	–15.05	–14.44	–15.32	–15.15	–15.45	–15.18	–14.82

whereas the other chair and the other two twist-boats have equatorial iodine. An outline of the calculation results is given in Table 2.

Surprisingly, not all of the calculation methods were able to find all the conformers as energy minima. All of the methods

found the two chairs as energy minima, but none of them were able to recognize all the twist-boat conformers. In addition, the energy values found for the conformers do not follow a particular pattern. In this respect, all of the methods suggest a conformational equilibrium in which two or more conformers are present in substantial amounts, but agreement was not reached as to which conformers are relevant or to the nature of the absolute minimum energy conformation. Depending on the calculation method, boat 2, chair 1, or chair 2 was found to be the lowest-energy conformation. Assessment of the calculated energy values for the aforementioned most stable conformations shows that none of them can be discarded as they are relevant in the equilibrium according to all calculation methods. On the other hand, the calculated energies suggest that both twist-boats **1** are rather insignificant in terms of the conformational ratios.

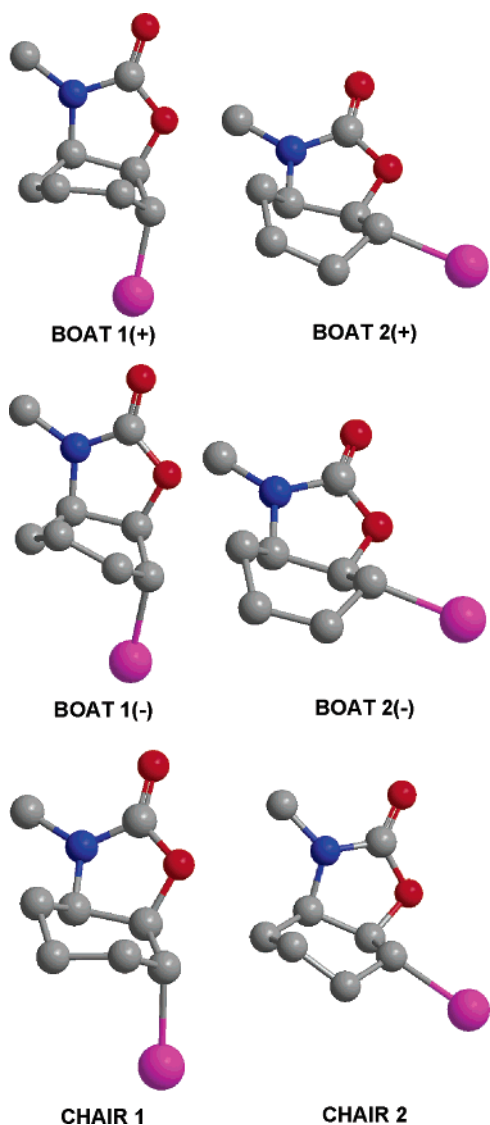
The geometries predicted by each method for the same conformation, mainly dihedral angles, are similar. The dihedral angles of all the minimum energy conformations found with all the theoretical methods are given in several tables in the Supporting Information. When these structural data are considered overall, the degree of similarity varies markedly depending on the conformation. Thus, the geometry found by all methods for both chairs is practically identical whereas the geometry found for the twist-boat conformations varies slightly. This variation cannot be properly assessed from the values of the dihedral angles but is significant statistically (vide infra).

The theoretical coupling constants were calculated from the dihedral angles using the Karplus-type equation of Haasnoot published 25 years ago.<sup>10</sup> This equation has been successfully applied to predict coupling constants from dihedral angles within an error of 0.5 Hz. The theoretical coupling constants for the minimum energy conformations found with all the theoretical methods can be found in the Supporting Information.

Having determined the experimental coupling constant ( $J_{\text{exp}}$ ) for the fourteen dihedral angles and the theoretical coupling constants ( $J_i$ ) for every angle in each conformation, the conformational equilibrium composition ( $x_i$ ) in a given solvent can be obtained by resolving an equation system formed by fourteen equations, eq 2, one for each experimental three-bond coupling constant, and eq 3.<sup>11</sup>

$$J_{\text{exp}} = x_1J_1 + x_2J_2 + x_3J_3 + \dots + x_nJ_n \quad (2)$$

$$x_1 + x_2 + x_3 + \dots + x_n = 1 \quad (3)$$

**FIGURE 2.** Minimum energy conformations of compound **2**.

**TABLE 2.** Relative Energies (kcal/mol) and Populations (%) of the Minimum Energy Conformations Found by Several Methods in the Theoretical Conformational Analysis

		conformations					
		boat 1(-)	boat 1(+)	boat 2(-)	boat 2(+)	chair 1	chair 2
MM2	$\Delta E$	1.57	—	—	0	0.91	0.91
	population	4.7	—	—	66.7	14.3	14.3
MM+	$\Delta E$	1.54	1.51	0.30	—	0.39	0
	population	3.3	3.4	26.5	—	22.8	44.0
AM1	$\Delta E$	—	0.51	0.44	0	1.18	0.49
	population	—	17.2	19.2	40.4	5.5	17.6
PM3	$\Delta E$	—	—	—	1.17	1.48	0
	population	—	—	—	11.4	6.7	81.9
MNDO	$\Delta E$	—	0.02	—	0	0.57	0.89
	population	—	37.7	—	38.9	14.8	8.6
B3LYP (LanL2DZ)	$\Delta E$	1.48	1.45	—	2.12	0	0.86
	population	5.7	6.0	—	1.9	69.9	16.4

**TABLE 3.** Mole Fractions,  $x_i$ , of 1 in Different Solvents from Eqs 2 and 3 Using the MM2-Derived Geometries of 2

	boat 1(-)	boat 2(+)	chair 1	chair 2	$R^a$	SEF <sup>a</sup>
acetic acid	0.03 ± 0.03	0.13 ± 0.03	0.17 ± 0.03	0.67 ± 0.03	0.9802	0.569
acetone	0.03 ± 0.04	0.12 ± 0.03	0.04 ± 0.04	0.81 ± 0.03	0.9847	0.632
acetonitrile	0.02 ± 0.04	0.11 ± 0.03	0.07 ± 0.03	0.80 ± 0.04	0.9823	0.658
benzene	0.04 ± 0.06	0.11 ± 0.05	0.17 ± 0.05	0.67 ± 0.05	0.9400	0.936
chloroform	0.03 ± 0.04	0.09 ± 0.03	0.31 ± 0.03	0.57 ± 0.03	0.9673	0.617
DMSO	0.02 ± 0.04	0.13 ± 0.03	0.03 ± 0.03	0.82 ± 0.04	0.9842	0.647
methanol	0.03 ± 0.03	0.12 ± 0.03	0.09 ± 0.03	0.76 ± 0.03	0.9838	0.60
pyridine	0.03 ± 0.04	0.13 ± 0.03	0.07 ± 0.03	0.77 ± 0.04	0.9816	0.643
CCl <sub>4</sub>	0.05 ± 0.03	0.06 ± 0.02	0.39 ± 0.03	0.50 ± 0.03	0.9704	0.520
toluene	0.02 ± 0.05	0.11 ± 0.04	0.21 ± 0.04	0.66 ± 0.05	0.9462	0.841
acetic acid		0.13 ± 0.03	0.18 ± 0.03	0.69 ± 0.03	0.9787	0.563
acetone		0.13 ± 0.03	0.06 ± 0.03	0.81 ± 0.03	0.9835	0.626
acetonitrile		0.12 ± 0.03	0.08 ± 0.03	0.80 ± 0.03	0.9820	0.633
benzene		0.12 ± 0.05	0.18 ± 0.05	0.70 ± 0.04	0.9360	0.913
chloroform		0.10 ± 0.03	0.31 ± 0.03	0.59 ± 0.03	0.9643	0.615
DMSO		0.14 ± 0.03	0.03 ± 0.03	0.83 ± 0.04	0.9840	0.621
methanol		0.12 ± 0.03	0.10 ± 0.03	0.78 ± 0.03	0.9831	0.584
pyridine		0.13 ± 0.03	0.09 ± 0.03	0.78 ± 0.04	0.9808	0.626
toluene		0.12 ± 0.04	0.21 ± 0.04	0.67 ± 0.04	0.9450	0.810

<sup>a</sup>  $R$  and SEF are the correlation coefficient and the standard error of the fit, respectively.

Because the number of equations is larger than the number of variables, the calculation was performed using a multiple linear regression analysis that yielded the best value for the molar fraction ( $x_i$ ) of each conformation in each solvent. The calculation was performed for all 10 solvents. In addition, the conformational composition in every solvent was recalculated using every set of theoretical coupling constants obtained from each modeling method to assess the reliability of the calculations. As an example, the conformational composition found in each solvent adjusting the experimental coupling constants to the theoretical coupling constants obtained from the MM2 force-field conformations is shown in Table 3. Similar tables can be found in the Supporting Information with the conformational composition derived from the theoretical coupling constants obtained by the other calculation methods.

Initially, all four conformations were used for the calculation. The population of boat 1 was found to be almost negligible with an estimated error of the same magnitude as the value

obtained, and an F-test showed that boat 1 is statistically insignificant. The boat 1 conformation was therefore discarded, and the calculation was repeated using only the three most populated conformers. In this way, the correlation coefficient ( $R$ ) of the calculation drops slightly by ca. 0.1–0.4%. In most cases, these coefficients are higher than 0.97, which indicates a very good correlation. The standard error of the fit (SEF) for most solvents is in the region of 0.6 Hz, a value similar to the estimated error in the calculation of the theoretical coupling constants using the Haasnoot equation. The quality of the fitting calculation drops to some extent in benzene and toluene (correlation coefficients of ca. 0.94), although the reasons for this are not clear. However, the results for these two solvents are better when data from the B3LYP method are used.

Comparison of the mole fractions,  $x_i$ , of conformers obtained from different theoretical methods warrants further comment. First, the quality of the fitting process is different depending on the origin of the conformational data. For example, theoretical coupling constants derived from molecular mechanics (MM2 and MM+) and DFT (B3LYP) geometries give better correlation coefficients and standard errors in the fit of eq 2 than those obtained from semiempirical calculations (AM1, PM3, and MNDO). MNDO clearly gave the worst results, and this was followed by PM3. Although results from AM1 are better, they

(10) Haasnoot, C. A. G.; De Leeuw, F. A. A. M.; Altona, C. *Tetrahedron* **1980**, *36*, 2783.

(11) Fielding, L.; Clark, J. K.; McGuire, R. *J. Org. Chem.* **1996**, *61*, 5978. Samoshin, V. V.; Troyansky, E. I.; Demchuk, D. V.; Ismagilov, R. F.; Chertkov, V. A.; Lindeman, S. V.; Khrustalyov, V. N.; Struchkov, Y. T. *J. Phys. Org. Chem.* **1998**, *11*, 241.

are inferior to those given by molecular mechanics and DFT, both of which are comparable.

Overall, boat 1(+) and boat 1(−) are hardly populated (see Table 2). Nevertheless, for each solvent system, they give different results in the calculation of the conformational distribution by eqs 3 and 4. Only MM+ and B3LYP yielded both conformers as local minima, and therefore, direct comparison of the mole fractions of the two boat forms is only possible using coupling constants obtained from these methods. In both cases, boat 1(−) is not detected at all by eq 2 whereas boat 1(+) has a rather small population in some solvents. Similar results were obtained by other minimization methods (see tables in the Supporting Information). In most solvents, the error in the calculation is equal to or greater than the population value of boat 1. In such cases, the fitting process was recalculated with this conformation discarded (see bottom of Table 3).

In general, all minimization methods predict at least one of the two boat 2 conformers to be significant in the equilibria. However, in the calculation of the conformational composition in each solvent (eqs 2 and 3) both boat 2 conformations behave in a similar way becoming nearly interchangeable. For instance, when AM1 conformers are used, differences were not found when the theoretical coupling constants derived from either the two conformers or one of them were used in the fitting calculation. This behavior can be ascribed to the similarity of the geometries obtained by AM1. Curiously, MM2 and B3LYP predict boat 2(+) as the only twist-boat conformer, whereas MM+ predicts only boat 2(−). Although their geometries are rather different, both boat 2 conformations have similar population values with similar correlation coefficients in the fitting of eqs 2 and 3. To assess the prevalence of one of these conformers, a fitting calculation (eqs and 3) was performed using boat 2(−) from MM+, boat 2(+) from B3LYP, and both chairs as the equilibrium conformers. The results of this analysis are very interesting. In all solvents, the population found for boat 2(+) was insignificant. Although this result must be interpreted carefully, the calculation recognizes boat 2(−) as the “true” conformer. However, such a conformation was not detected as a minimum by MM2, B3LYP, PM3, or MNDO. A plausible explanation is that the potential energy surface between the two twist-boat conformers is rather “flat”; i.e., the barrier existing between them is low enough to be easily overcome by the calculation algorithms. In addition, on considering the graphical representation of the conformers (see Figure 2), the small twisting of boat 2(−) and boat 2(+) from the boat conformation can easily be seen. In any case, because both twist-boats have the same population and can be exchanged when treated separately, they will henceforth be referred to as boat 2.

The most populated conformer is chair 2, and this ranges between 50 and 52% in the least polar solvent (carbon tetrachloride) and 83% in the most polar solvents (DMSO and acetone). The mole fraction of chair 1 is also significant in several solvents, ranging from 39% in carbon tetrachloride to less than 5% in DMSO or acetone. Finally, the amount of the boat 2 conformation seems to be nearly constant at a level slightly above 10%. These results are highly consistent regardless of the modeling method and the nature of the conformers used in the fitting calculation. Indeed, MM2, MM+, and B3LYP gave almost identical results.

To assess the influence of the solvent in the equilibrium and find a possible predictive mathematical equation to describe such

**TABLE 4.** Calculated Conformational Composition in the Measured Solvents from Eqs 3, 5, and 6

	$\pi^*$	$\alpha$	$\beta$	boat 2	chair 1	chair 2
acetic acid	0.64	1.12	0.00	0.11	0.19	0.70
acetone	0.71	0.08	0.48	0.12	0.08	0.82
acetonitrile	0.75	0.19	0.31	0.12	0.10	0.81
benzene	0.59	0.00	0.10	0.10	0.19	0.71
chloroform	0.58	0.44	0.00	0.10	0.23	0.67
DMSO	1.00	0.00	0.76	0.15	0.03	0.90*
methanol	0.60	0.93	0.62	0.11	0.10	0.80
pyridine	0.87	0.00	0.64	0.14	0.10	0.79
CCl <sub>4</sub>	0.28	0.00	0.00	0.06	0.41	0.53
toluene	0.54	0.00	0.11	0.09	0.21	0.68

an equilibrium, several correlations with known solvent parameters were performed.

First, only the three most populated conformers (chair 2, chair 1, and boat 2) were used to simplify the calculation. In addition, only results obtained from MM2, MM+, and B3LYP were used. The solvent parameters used were those of Kamlet and Taft, where the explicit parameters represent the ability of the solvent to stabilize a charge or a dipole by virtue of its dielectric effect ( $\pi^*$ ) and the ability of the solvent to behave as a hydrogen-bond donor ( $\alpha$ ) or hydrogen-bond acceptor ( $\beta$ ). Values of these parameters in different solvents are given in the literature and are presented in Table 4.<sup>9</sup>

The equilibrium constants between the conformational species defined as  $[\text{chair2}]/[\text{chair1}]$  and  $[\text{chair1}]/[\text{boat2}]$  can be obtained from the data in Table 3 (and similar tables in the Supporting Information). These equilibrium constants are strongly influenced by the solvent. This influence can be quantified using eq 4, a modification of the Kamlet and Taft multiparameter treatment, where 0.59, 0.0, and 0.1 are the values for  $\pi^*$ ,  $\alpha$ , and  $\beta$  of the reference solvent benzene and  $\log([\text{sp.A}]/[\text{sp.B}])_o$  refers to the species in a given equilibrium in this solvent.

$$\log\left(\frac{[\text{sp.A}]}{[\text{sp.B}]}\right) = \log\left(\frac{[\text{sp.A}]}{[\text{sp.B}]}\right)_o + s(\pi^* - 0.59) + a(\alpha - 0.0) + b(\beta - 0.1) \quad (4)$$

Several multiple regression analyses were investigated using all the possible combinations of the solvatochromic parameters. The standard error of the fitting and an F-test were used as criteria to determine the number and type of parameters that were statistically significant in each case. In this way, eqs 5 and 6 were obtained:

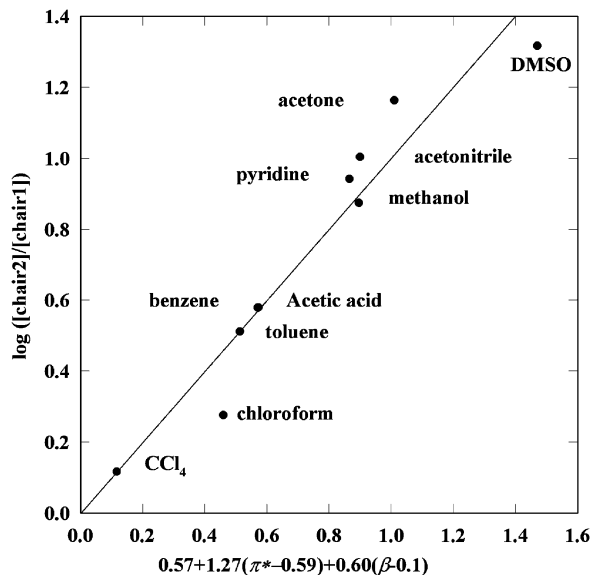
$$\log\left(\frac{[\text{chair2}]}{[\text{chair1}]}\right) = (0.571 \pm 0.02) + (1.27 \pm 0.1)(\pi^* - 0.59) + (0.60 \pm 0.1)(\beta - 0.1) \quad (5)$$

where  $R = 0.943$  and the standard error of the fit = 0.13, and

$$\log\left(\frac{[\text{chair1}]}{[\text{boat2}]}\right) = (0.276 \pm 0.03) - (1.55 \pm 0.1)(\pi^* - 0.59) - (0.53 \pm 0.1)(\beta - 0.1) \quad (6)$$

where  $R = 0.94$  and the standard error of the fit = 0.15. The best statistical result shows that the solvent effect on the equilibria described here involves only the dipolarity, polarizability ( $\pi^*$ ), and hydrogen-bond acceptor (HBA) property ( $\beta$ ) of the solvent.

A plot of  $\log[\text{chair2}]/[\text{chair1}]$  vs the calculated value from eq 5 can be seen in Chart 1. A good linearity can be observed,

**CHART 1.** Comparison between the Experimental and Calculated (from Eq 5)  $\log([\text{chair}2]/[\text{chair}1])$  Values

and this suggests an excellent predictive value. Note that benzene and acetic acid are at the same point.

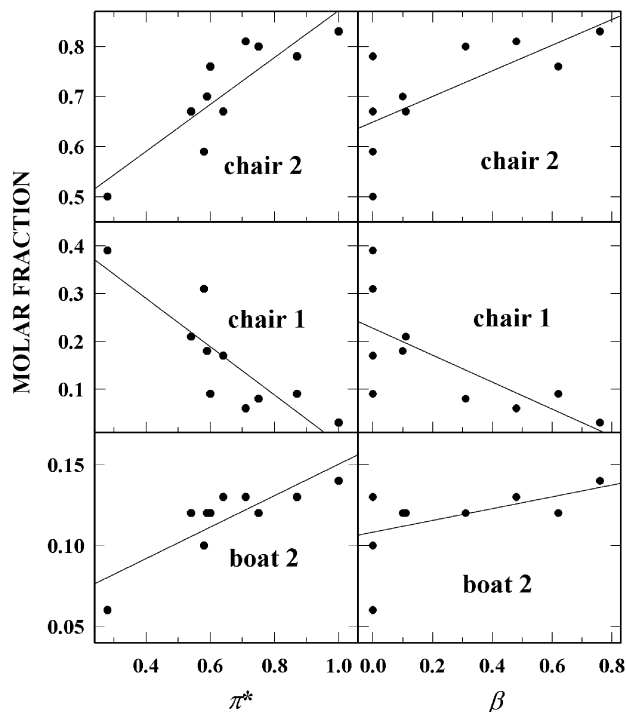
From the right side of eqs 5 and 6, the mole fractions of the individual conformers chair 1, chair 2, and boat 2 can be calculated. These values, shown in Table 4, compare favorably with those obtained experimentally (Table 3). The differences in acetone and DMSO can easily be attributed to the small value of chair 1 in such solvents, which makes difficult the approximation of the results.

It is also possible to analyze the individual behavior of each solvent property in the conformational equilibria. A plot of the molar fraction of each conformation vs  $\pi^*$ , the solvent parameter related to the polarity, can be adjusted to the most probable straight line. The slope of this line gives a quantitative way of assessing the variation of the molar fraction of each conformation with the polarity of the solvent. These lines are shown in Chart 2.

It can be seen that the molar fractions of chair 2 and boat 2 increase in the more polar solvents, with chair 2 changing strongly and boat 2 changing only slightly. On the other hand, the molar fraction of chair 1 decreases. The respective slope values can be seen in the first column of Table 5. These data clearly indicate that an increase in the solvent polarity causes a significant increase in the population of chair 2 and, to a lesser extent, the population of boat 2. These increases are concomitant with a rapid reduction in the population of chair 1.

A similar numerical treatment can be performed for the three molar fractions of the conformations and the parameter  $\beta$ , which is associated with the ability of the solvent to act as a hydrogen-bond acceptor (see Chart 2). In this case, when  $\beta$  increases, the concentration of chair 1 diminishes moderately and the concentration of chair 2 increases by roughly the same value. The concentration of boat 2 remains virtually unchanged. The numerical values for the slope are presented in the second column of Table 5.

The effect of polarity can be separated from the effect of hydrogen-bonding interactions by restraining the correlation to solvents with a value of  $\beta = 0$ . Likewise, analysis of the hydrogen-bonding interaction can be separated from the polarity effect by using solvents with a value similar to the polarity

**CHART 2.** Molar Fraction of Each Conformation vs  $\pi^*$  and  $\beta$ **TABLE 5.** Slopes of the Individual Correlations between Each Solvent Parameter and Each Conformer Concentration

	$\pi^{*a}$	$\beta^a$	$\pi^{*b}$	$\beta^b$
chair 2	+0.47	+0.26	+0.47	+0.26
chair 1	-0.50	-0.28	-0.52	-0.28
boat 2	+0.10	+0.04	+0.10	+0.01

<sup>a</sup> Values obtained with all the solvents. <sup>b</sup> Values obtained with selected solvents ( $\beta = 0$ ).

parameter; for instance,  $0.5 < \pi^* < 0.7$ . The slopes calculated in this way are shown in the third and fourth columns of Table 5 and are very similar to those calculated with all the data values.

In conclusion, a complex system of conformational equilibria in 10 solvents was analyzed by means of theoretically determined geometries and by resolving the time-averaged NMR H–H coupling constants into contributions from several conformers using a Karplus-type treatment. The major conformations were a boat and two chair forms, the mole fractions of which correlated with the polarity–polarizability and HDB properties of the solvents. This approach can be useful because the correlation with solvent properties allows prediction of the equilibrium distribution of conformers of **1** in additional solvents.

## Experimental Section

<sup>1</sup>H NMR experiments in 10 different solvents (acetic acid-*d*<sub>4</sub>, acetone-*d*<sub>6</sub>, acetonitrile-*d*<sub>3</sub>, benzene-*d*<sub>6</sub>, CCl<sub>4</sub>, CDCl<sub>3</sub>-*d*<sub>3</sub>, DMSO-*d*<sub>6</sub>, MeOH-*d*<sub>4</sub>, pyridine-*d*<sub>5</sub>, and toluene-*d*<sub>8</sub>) were acquired at 400 MHz. In the case of CCl<sub>4</sub>, a coaxial insert with DMSO-*d*<sub>6</sub> was used as the field lock. Compound ( $\pm$ )-**1** was previously synthesized in our laboratory from ( $\pm$ )-*N*-(3-cyclohexenyl)-*N*-benzylamine by reaction with CO<sub>2</sub> and I<sub>2</sub>.<sup>12</sup>

(12) García-Egido, E.; Marcos, M.; Carballo, R.; Muñoz, L. *J. Mol. Struct.* **2000**, 524, 233.

**Determination of  $J_{\text{exp}}$ .** The homonuclear H–H experimental coupling constant values ( $J_{\text{exp}}$ ) and the chemical shifts ( $\delta$ ) of protons belonging to the cyclohexane ring were determined through the classical method of multiplet resolution through simulation and iteration of the experimental monodimensional  $^1\text{H}$  NMR spectrum in each solvent by means of the LAOCOON-type program g-NMR.<sup>13</sup> Each  $^1\text{H}$  NMR spectrum was acquired with 64 K data points and Fourier transformed with zero filling. A Gaussian function was applied to the FID before transformation to increase resolution.

**Molecular Modeling.** Compound **2** was modeled at different levels of theory in the gas phase to find all the possible conformers. Initially, a search of all possible relevant chair and twist-boat conformations was manually done. As a result, two chair and four twist-boat conformations were used as starting conformations. Molecular mechanics calculations were performed with the MM2<sup>14</sup> force field contained in the ChemBats3D package<sup>15</sup> and with the MM+ force field included in HYPERCHEM 7.04.<sup>16</sup> Calculations at the semiempirical level of theory were carried out with MNDO, AM1,<sup>17</sup> and PM3.<sup>18</sup> Finally, a calculation was performed at the ab initio level of theory using a hybrid DFT method, B3LYP with the D95V basis set except for I, for which the LanL2DZ<sup>19</sup> pseudo-potential was used for the sake of affordability. When energy

optimizations were carried out for every starting conformation, not all the methods provided a consistent conformational space. This fact suggested us to perform a systematic analysis of the accuracy obtained with these different methods (see below).

**Determination of Three-Bond Theoretical Coupling Constants ( $J_{\text{T}}$ ).** Theoretical coupling constant values ( $J_{\text{T}}$ ) were estimated for every conformation from dihedral angles obtained by molecular modeling by using the Karplus-type equation developed by Haasnoot et al. (eq 7).<sup>10</sup> In this equation,  $\phi$  is the torsion angle,  $\Sigma\Delta\chi_i$  is the sum of the electronegativity differences between each substituent and a proton ( $\Delta\chi_i = \chi_{\text{sust}} - \chi_{\text{H}}$ ),  $\xi_i$  gives the relative orientation of each substituent, and  $P_1$ – $P_6$  are empirical parameters.

$${}^3J_{\text{HH}} = P_1 \cos^2 \phi + P_2 \cos \phi + P_3 + \Sigma\Delta\chi_i \{P_4 + P_5 \cos^2(\xi_i\phi + P_6|\Sigma\Delta\chi_i|)\} \quad (7)$$

**Acknowledgment.** J.L.L. thanks the Junta de Andalucía (FQM-171) for financial support. E.V. is grateful to the Xunta de Galicia for a fellowship. L.M. thanks the Ministerio de Educación (BQU2002-02807) and the Xunta de Galicia (PGIDIT03PXIC30107PN) for financial support.

**Supporting Information Available:** Results of conformational distribution, dihedral angles, and coupling constants obtained from molecular modeling at different levels of theory in the gas phase: molecular mechanics calculations (MM2 and MM+), semiempirical calculations (MNDO, AM1, PM3), and DFT calculations (B3LYP Lan2DZ) described in the text. Energies and Cartesian coordinates of the six conformers. Experimental and simulated spectra of compound **1** in acetone. This material is available free of charge via the Internet at <http://pubs.acs.org>.

JO051917P

(13) Budzelaar, P. H. M. *gNMR*, version 4.1; Cherwell Scientific Ltd. Castellano, S.; Bothner-By, A. A. *J. Chem. Phys.* **1964**, *41*, 3863.

(14) (a) Allinger, N. L. *Adv. Phys. Org. Chem.* **1976**, *13*, 1–82. (b) Burkert, U.; Allinger, N. L. *Molecular Mechanics*, ACS Monograph No. 177, American Chemical Society: Washington, D.C., 1982.

(15) *ChemBats3D*, version 5.0; CambridgeSoft Corporation.

(16) *Hyperchem for windows*, release 7.04; Hypercube, Inc.

(17) Dewar, M.; Thiel, W. *J. Am. Chem. Soc.* **1977**, *99*, 2338.

(18) Stewart, J. J. P. *J. Comput. Chem.* **1989**, *10*, 209.

(19) Hay, P. J.; Wadt, W. R. *J. Chem. Phys.* **1985**, *82*, 270. Wadt, W. R.; Hay, P. J. *J. Chem. Phys.* **1985**, *82*, 284. Wadt, W. R.; Hay, P. J. *J. Chem. Phys.* **1985**, *82*, 299.